JB&JS OPEN ACCESS

Femoral Nailing in a Porcine Model Causes Bone Marrow Emboli in the Lungs and Systemic Emboli in the Heart and Brain

Steinar Kristiansen, MD, Anders Hagen Jarmund, MSc, Jonas Hilmo, MD, Tom Eirik Mollnes, MD, PhD, Martin Leth-Olsen, MD, Siri Ann Nyrnes, MD, PhD, Bent Aksel Nilsen, RN, Renathe Henriksen Grønli, MSc, Bjørn Ove Faldaas, MSc, Benjamin Storm, MD, PhD, Arild Espenes, DVM, PhD, and Erik Waage Nielsen, MD, PhD

Background: Shaft fractures of the femur are commonly treated with intramedullary nailing, which can release bone marrow emboli into the bloodstream. Emboli can travel to the lungs, impairing gas exchange and causing inflammation. Occasionally, emboli traverse from the pulmonary to the systemic circulation, hindering perfusion and resulting in injuries such as heart and brain infarctions, known as *fat embolism syndrome*. We studied the extent of systemic bone marrow embolization in a pig model.

Methods: Twelve anesthetized pigs underwent bilateral intramedullary nailing of the femur, while 3 animals served as sham controls. Monitoring included transesophageal echocardiography (TEE), pulse oximetry, electrocardiography, arterial blood pressure measurement, and blood gas and troponin-I analysis. After surgery, animals were monitored for 240 minutes before euthanasia. Post mortem, the heart, lungs, and brain were biopsied.

Results: Bone marrow emboli were found in the heart and lungs of all 12 of the pigs that underwent intramedullary nailing and in the brains of 11 of them. No emboli were found in the sham group. The pigs subjected to intramedullary nailing exhibited significant hypoxia (PaO_2/FiO_2 ratio, 410 mm Hg [95% confidence interval (CI), 310 to 510) compared with the sham group (594 mm Hg [95% CI, 528 to 660]). The nailing group exhibited ST-segment alterations consistent with myocardial ischemia and a significant increase in the troponin-I level compared with the sham group (1,580 ng/L [95% CI, 0 to 3,456] versus 241 ng/L [95% CI, 0 to 625] at the 240-minute time point; p = 0.005). TEE detected emboli in the right ventricular outflow tract, but not systemically, in the nailing group.

Conclusions: Bilateral intramedullary nailing caused bone marrow emboli in the lungs and systemic emboli in the heart and brain in this pig model. The observed clinical manifestations were consistent with coronary and pulmonary emboli. TEE detected pulmonary but not systemic embolization.

Clinical Relevance: Femoral intramedullary nailing in humans is likely to result in embolization as described in our pig model. Focused monitoring is necessary for detection of fat embolism syndrome. Absence of visual emboli in the left ventricle on TEE does not exclude the occurrence of systemic bone marrow emboli.

During orthopaedic surgery or bone fractures, bone marrow can cause pulmonary emboli[1]. Some emboli may pass to the systemic circulation, leading to fat embolism syndrome[1]. Bone marrow emboli consist of white (fatty) and red (cell-rich) bone marrow. Up to 35% of patients with bone marrow embolism develop respiratory failure or heart or brain infarction[2-4]. Risk factors include young age, male sex, and long-bone fracture[5-7]. Mortality rates range from 8.3% to 17.6% and are highest in elderly patients with femoral neck fracture[8]. Early diagnosis and organ support reduce mortality[3,9]. Emboli reaching the brain may cause neurological symptoms and increased intracranial pressure necessitating decompressive neurosurgery[10-13], with the potential for complete recovery[14-16].

Diagnosing fat embolism syndrome is challenging, with uncertain accuracy of clinical scoring systems[1,17] based on

Disclosure: The study received funding from Helse Nord, the Odd Berg Group, The Royal Norwegian Society of Sciences and Letters, and the Blix Family Fund. The Article Processing Charge for open access publication was funded by The Arctic University of Norway (UiT). The **Disclosure of Potential Conflicts of Interest** forms are provided with the online version of the article (http://links.lww.com/JBJSOA/A606).

JBJS Open Access • 2024:e23.00128 openaccess.jbjs.org

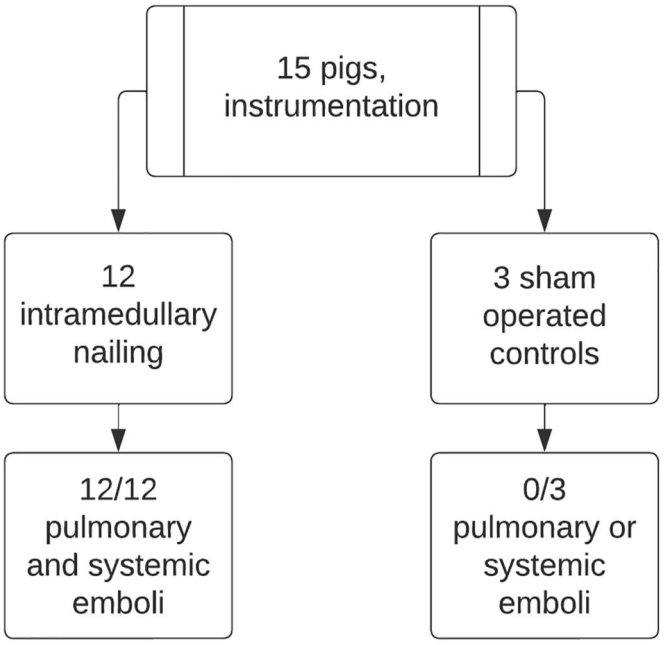

Fig. 1

Allocation of pigs and distribution of emboli. Fifteen pigs were included: 12 allocated to intramedullary reaming and 3 allocated to the sham group.

inflammation, neurological symptoms, petechiae, and respiratory failure. Cerebral magnetic resonance imaging (MRI) with susceptibility- and diffusion-weighted images is definitive for diagnosing cerebral bone marrow emboli[4,18-20], while computed tomography (CT) is insufficient for diagnosing cerebral and pulmonary emboli[21,22]. Perioperative transesophageal echocardiography (TEE) can detect emboli[23-26] but is rarely used during orthopaedic surgery. Histopathological examination, including oil red-O staining, detects emboli in tissue biopsy specimens[27]. Systemic embolization during orthopaedic surgery has been reported[10,11,28-30] but has to our knowledge not been systematically examined. Therefore, we assessed the extent of systemic embolization during intramedullary nailing in a pig model using assessment of clinical deterioration, TEE, electrocardiography (ECG), and postmortem biopsies.

Materials and Methods

Animals

Our study included 15 specific pathogen-free Norwegian Landrace pigs (average weight, 27.0 kg; standard deviation [SD], 4 kg); 12 underwent intramedullary reaming and nailing and 3 served as sham controls (Fig. 1). Exclusion criteria were preexisting disease, unexpected complications unrelated to the intramedullary nailing, and a patent foramen ovale; no animals were excluded. The study was approved by the Norwegian Animal Welfare Committee (FOTS-ID#19803) and European Union directive 2010/63/EU.

Instrumentation, Anesthesia, and Monitoring

An overview of the instrumentation used for the intramedullary nailing is provided in Figure 2. All 15 pigs were anesthetized using intramuscular azaperone (40 mg), ketamine (500 mg), and atropine (0.5 mg). A peripheral venous catheter was placed in an ear vein bilaterally. Pentobarbital was titrated to maintain

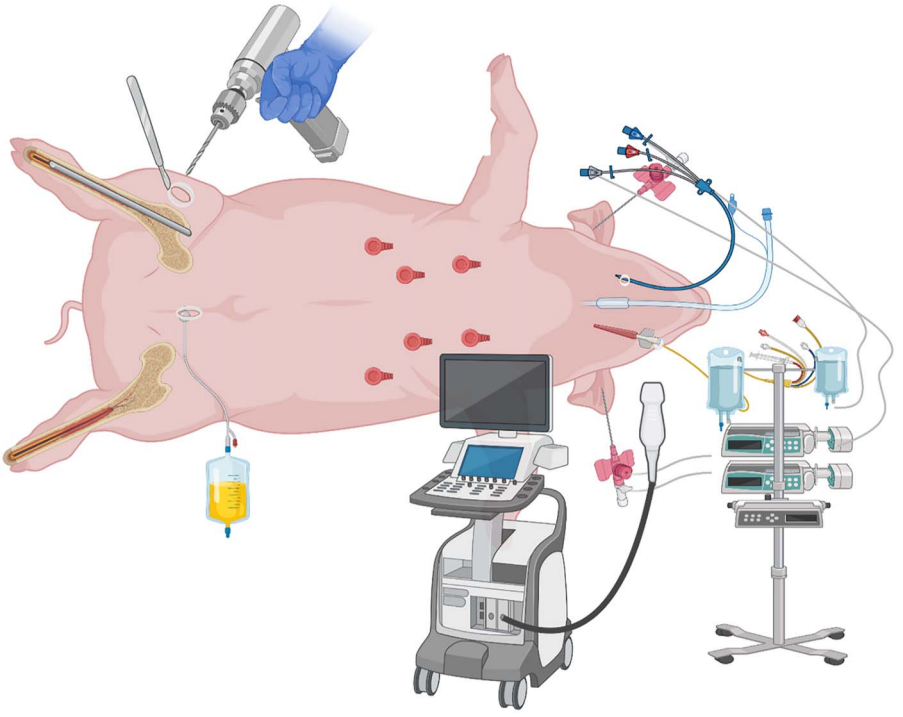

Fig. 2

Overview of instrumentation in the pigs undergoing intramedullary reaming and nailing.

spontaneous breathing and sufficient anesthesia. We intubated the pigs endotracheally using a 7.0-mm-outer-diameter tube.

We maintained anesthesia with intravenous morphine (2 mg/kg/hr), midazolam (0.15 mg/kg/hr), and pentobarbital (4 mg/kg/hr). The animals were ventilated with a tidal volume of 10 to 13 mL/kg, respiratory rate of 20 to 24/min, and positive end-expiratory pressure of 5 cm H_2O. Ventilation was titrated to a pH of 7.4 ± 0.5, and the fraction of inspired oxygen (FiO_2) was adjusted to maintain the arterial pulse oximetry saturation (SpO_2) above 90%. Ringer acetate solution was infused (8 to 10 mL/kg/hr). When the mean arterial pressure (MAP) dropped below 50 mm Hg, we administered 2-mL/kg boluses of Ringer acetate solution and a noradrenaline infusion was started at 0.05 μg/kg/min and titrated to achieve an MAP above 50 mm Hg. Noradrenaline (1 μg/kg) was administered if the MAP dropped below 45 mm Hg.

We placed a 4-Fr 8-cm arterial catheter (PiCCO; Pulsion/Getinge) in the right carotid artery and a 7-Fr 15-cm central venous catheter (Certofix Trio; B. Braun) in the right external jugular vein with an ultrasound-guided technique. A heparin flush solution (2.5 IU/mL) was used to avoid coagulation. We placed a suprapubic catheter with a temperature sensor in the bladder. A pediatric 9-T TEE probe (GE Healthcare) was positioned in the upper esophageal position and connected to an echocardiography machine (Vivid 7; GE Vingmed). We installed a NeoDoppler ultrasound probe (NeoDoppler research setup[31], Norwegian University of Science and Technology) after an approximately 1 × 2-cm trepanation for monitoring cerebral blood flow. We used 6-lead ECG with monitoring of ST-segment changes, SpO_2, end-tidal CO_2, and continuous invasive arterial and central venous pressures (IntelliVue MP70; Phillips) to monitor for ischemia, defined as at least 1 of the following: (1) ST-segment depression exceeding 1 mm at the J point in ≥2 contiguous leads, (2) ST-segment elevation exceeding 1 mm at the J point in ≥2 contiguous limb leads, and/or (3) ST-segment elevation exceeding 2 mm in ≥2 contiguous precordial leads.

Preoperatively, we performed TEE with agitated saline solution to rule out a patent foramen ovale. The probe was then positioned as described by Vik et al.[32] and Storm et al.[33] for visualization of the aorta or left ventricular outflow tract (LVOT) and pulmonary artery or right ventricular outflow tract (RVOT) for continuous ECG. TEE was performed before, during, and after intramedullary nailing (or approximately 30 minutes after instrumentation in the sham group).

After anesthesia, instrumentation, and preoperative monitoring, the pigs were assigned to either undergo bilateral intramedullary nailing of the femur (n = 12) or not undergo surgery (sham group; n = 3). About 240 minutes after completion of the intramedullary nailing or after completion of the instrumentation in the sham group, we killed the animals by central venous injection of potassium chloride.

Blood and Tissue Sampling and Analyses

Blood was collected from the carotid artery before surgery, after completion of bilateral intramedullary nailing (or 30 minutes after the arterial catheter was placed in the sham group), and 2 and 4 hours after the surgery or after arterial cannulation in the sham group.

We sampled a total of 75 mL of blood per animal, using a Vacutainer (BD) closed vacuum system and serum tubes with clot activator and gel (VACUETTE; Greiner Bio-One) for serum samples, and a *safe*PICO syringe with heparin (Radiometer) for arterial blood gas analysis. To avoid pre-analysis heparin contamination from the line flush solution, 4 mL of blood was withdrawn and discarded before sampling. After 30 minutes of clotting, the serum was centrifuged at 2,000 ×g for 10 minutes, transferred to cryotubes, and stored at −80°C for analysis. Arterial blood gases were analyzed immediately.

We analyzed troponin-I levels using an Atellica IM analyzer (Siemens Healthineers, Siemens Healthcare) and arterial blood gases using an ABL80 FLEX blood gas analyzer (Radiometer).

Post mortem, we biopsied the lungs, heart, and brain, and examined for an intracardiac shunt.

Orthopaedic Surgery

An orthopaedic surgeon performed all orthopaedic procedures. With the pigs in a lateral position, a longitudinal incision was made from approximately 5 cm distal to 5 cm proximal to the proximal border of the femur. The trochanteric fossa was identified, and the medullary canal was opened with a drill bit. A guidewire was inserted, and the canal was opened with an entry reamer (Bixcut IM Reamer; Stryker). Sequential reaming was performed from 6.5 to 11 or 11.5 mm in increasing increments of 0.5 mm. A trochanteric antegrade nail (TRIGEN TAN; Smith & Nephew) with a diameter of 10 mm was cut to a length of 15 cm, longer than the femur for easy removal. The distal part of the nail was then inserted. The incision was closed with a stapler, and the procedure was repeated on the contralateral side.

Histopathological Analyses

Tissue samples of the brain, lungs, and heart measuring 1 × 1 × 0.3 cm were frozen in optimal cutting temperature (O.C.T.) compound (Tissue-Tek; Sakura) on dry ice. Tissue slices of 8 μg were cut at −20°C using a Leica CM1950 cryostat (Leica Biosystems). The slices were mounted on Superfrost Plus slides (Epredia) and air-dried, fixed with 4% neutral buffered formalin mixed with 63% ethanol for 5 minutes, dipped in 60% isopropanol for 2 minutes, and incubated in a 0.3% solution of oil red O (Sigma-Aldrich) (6 mL of 0.5% oil red O diluted with 4 mL of H_2O) for 10 minutes.

After incubation, samples were rinsed in 60% isopropanol and counterstained with Mayer's hematoxylin solution (Sigma-Aldrich) for 5 minutes, rinsed for 10 minutes under running tap water, and mounted with glycerol jelly. Images of oil red O-stained samples were captured using a Nikon DS-Fi3 camera (Nikon Systems) installed on a Nikon ECLIPSE Ci light microscope. The images were processed using NIS-Elements (Nikon).

We defined a positive biopsy as ≥2 intravascular or perivascular emboli stained with oil red O in the same section.

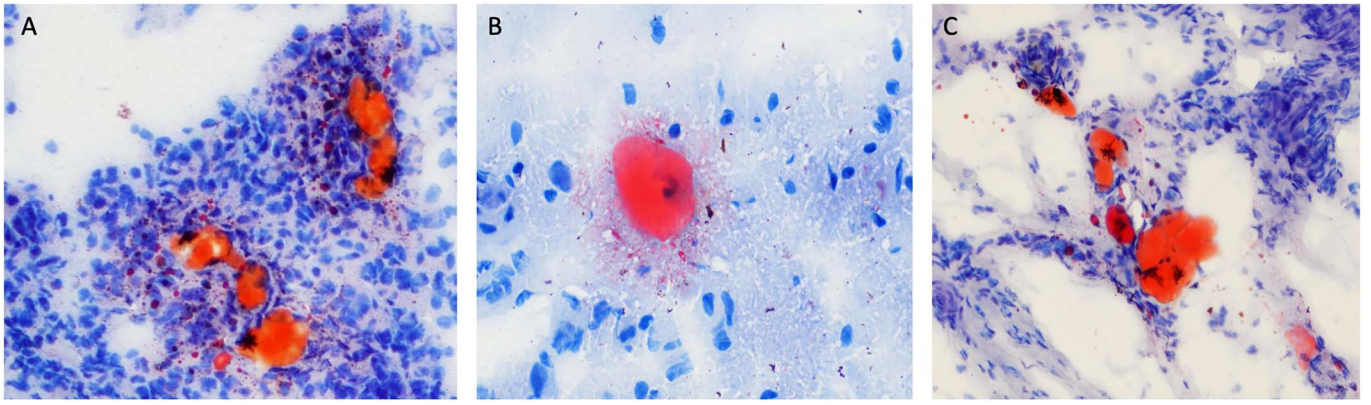

Fig. 3

Histopathologic examinations of tissue prepared in O.C.T. compound and frozen on dry ice revealed bone marrow emboli in cardiac (**Fig. 3-A**), cerebral (**Fig. 3-B**), and pulmonary cryosections (**Fig. 3-C**) with ×10, ×40, and ×10 magnification, respectively. Bone marrow emboli were stained red by the oil red O.

Power Calculation

We expected systemic bone marrow emboli in 70% of the pigs in the intramedullary nailing group and none in the sham group. Aiming for a power of 80%, an alpha of 5%, a beta of 20%, and an enrollment ratio of 0.3, we determined that allocation of 12 animals to the nailing group and 4 to the sham group (16 animals in total) was needed. However, we considered 3 animals sufficient for the sham group as bone marrow emboli are unlikely in animals that do not undergo an operation.

Statistical Analysis

Data are presented as the mean with the 95% confidence interval (CI). The lower CI limit for biological data, where the true mean cannot be below zero, was bounded at zero. We

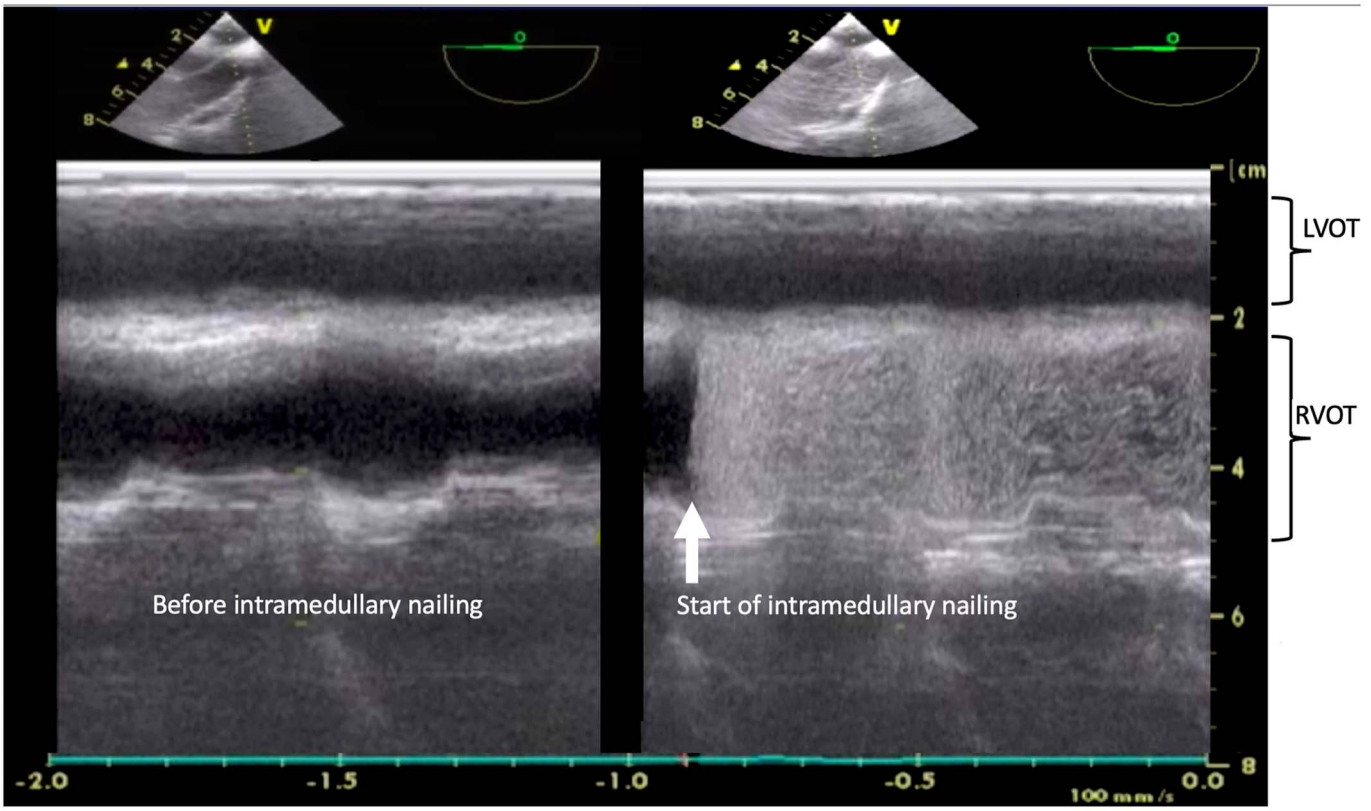

Fig. 4

Transesophageal echocardiography with an M-mode image showing the left and right ventricular outlet tracts (LVOT and RVOT, respectively) before (left image) and immediately after (right image) femoral intramedullary nailing. The x axis shows time in seconds, and the y axis shows depth in centimeters. Dense, hyperechogenic material filled the RVOT as intramedullary nailing commenced. No emboli were visible in the LVOT.

JBJS Open Access • 2024:e23.00128 openaccess.jbjs.org 5

TABLE I PaO_2/FiO_2 Ratio, MAP, and Troponin-I Levels*

	Mean (95% CI)			
	Sham (N = 3)	Intramedullary Nailing (N = 12)	Difference Between Intramedullary Nailing and Sham	P Value
PaO_2/FiO_2 ratio *(mm Hg)*				
30 minutes preop.	539 (429 to 649)	517 (427 to 606)	−22 (−223 to 189)	0.826
30 minutes postop.	594 (528 to 660)	410 (310 to 510)	−184 (−318 to −51)	0.011
MAP *(mm Hg)*				
30 minutes preop.	62 (52 to 69)	69 (62 to 77)	7 (0 to 26)	0.751
0 to 30 minutes postop.	70 (65 to 72)	66 (61 to 72)	4 (0 to 16)	0.211
Troponin-I level *(ng/L)*				
30 minutes preop.	162 (0 to 380)	350 (183 to 518)	188 (−153 to 529)	0.256
240 minutes postop.	241 (0 to 625)	1,580 (0 to 3,456)	1,339 (1,196 to 1,470)	0.005

*Preop. and postop. refer to before and after completed instrumentation in the sham group.

analyzed group differences using the Student unpaired t test or mixed models. $P < 0.05$ was considered significant.

Results

Bone marrow emboli were found in histopathological examinations of the lungs and hearts in all 12 pigs in the intramedullary nailing group and in the brains of 11 of them (Fig. 3). TEE showed bone marrow emboli in the RVOT during intramedullary reaming and nailing (Fig. 4) in all 12 pigs. No emboli were found in the pigs in the sham group.

On TEE, embolization was most intense during the reaming and nailing procedures, and the intensity gradually decreased before ceasing after the procedures were finalized. Emboli were visible on TEE before clinical deterioration, whereas no emboli were detected in the LVOT or aorta.

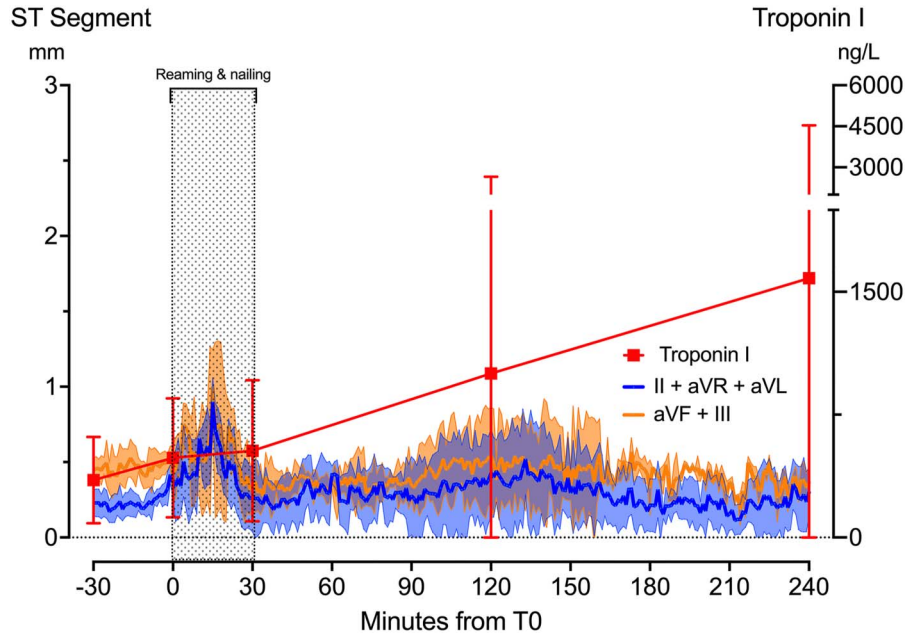

Fig. 5

Changes in the ST segment and troponin-I levels during monitoring. ST-segment changes at the J point, shown as millimeters of deviation from the J point, for the 12 animals undergoing bilateral femoral nailing revealed substantial ischemia, which was most pronounced during actual reaming and nailing. The blue line shows averaged ST-segment changes in ECG leads II, aVR, and aVL. The orange line shows averaged ST-segment changes in ECG leads aVF and III. The shaded areas cover ±1 SD. The mean troponin-I level (red line), shown in ng/L, increased throughout the experiment in all pigs undergoing femoral intramedullary nailing but varied considerably between the pigs. Error bars span ±1 SD. If a measurement minus 1 SD was negative, the lower error bar was bounded at zero.

Clinical Manifestations of Bone Marrow Emboli

Respiration and Ventilation

After arterial cannulation (30 minutes preoperatively), the PaO_2/FiO_2 ratio (partial pressure of oxygen in arterial blood relative to FiO_2) was 517 mm Hg (95% CI, 427 to 606) in the intramedullary nailing group compared with 539 mm Hg (95% CI, 429 to 649) in the sham group, a difference of −22 mm Hg (95% CI, −223 to 189; p = 0.826). After nailing, the PaO_2/FiO_2 ratio was 410 mm Hg (95% CI, 310 to 510) versus 594 mm Hg (95% CI, 528 to 660) in the sham group, a difference of −184 mm Hg (95% CI, −318 to −51; p = 0.011). End-tidal CO_2 did not differ significantly between the groups.

Hemodynamics and Cardiac Injury

Only animals exposed to intramedullary nailing experienced hemodynamic insults, including hypotension, ECG changes, and elevation of the troponin-I level (Table I). The preoperative MAP was 69 mm Hg (95% CI, 62 to 77) in the intramedullary nailing group and 62 mm Hg (95% CI, 52 to 69) in the sham group. There was no significant difference in the postoperative MAPs between the groups. However, 3 of the 12 experimental pigs exhibited an MAP below 35 mm Hg, with the lowest MAP in a single pig being 31 mm Hg and occurring 22 minutes after intramedullary nailing. These 3 pigs were treated with fluid and noradrenaline, which rapidly achieved an MAP above 50 mm Hg.

Four of the 12 pigs exhibited ST-segment elevation of >2 mm at the J point, indicative of myocardial ischemia, in leads II, III, and aVL. A clinically relevant change in the ST segment occurred as early as 4 minutes after initiation of reaming and persisted for an average of 26 minutes (95% CI, 15 to 37) (Fig. 5). One pig had persistent ECG signs of ischemia, and 2 had ST-segment depression of >1 mm in leads aVL and aVR, consistent with subendocardial ischemia.

The troponin-I level before intramedullary nailing averaged 350 ng/L (95% CI, 183 to 518), increasing to 1,580 ng/L (95% CI, 0 to 3,456) 240 minutes postoperatively (Fig. 5). In the sham animals, the troponin-I level averaged 162 ng/L (95% CI, 0 to 380) in the first sample taken after arterial cannulation and increased to 241 ng/L (95% CI, 0 to 625) after 240 minutes. The troponin-I level was significantly higher in the intramedullary nailing group compared with the sham group at all sampling points after the start of surgery (p = 0.040).

Six of the 12 pigs exposed to intramedullary reaming had a >50% increase in the troponin-I level between the first preoperative sample and the last sample taken 240 minutes after surgery, indicating myocardial infarction.

Discussion

Bilateral intramedullary nailing consistently caused bone marrow emboli in the lungs and heart in all 12 of the pigs in our experimental group and in the cerebral arteries of all but 1. Clinical findings indicated coronary and pulmonary emboli. This study highlights that bone marrow emboli can bypass the lungs and spread systemically to the heart and brain, a finding that is supported by previous evidence of physiological shunts in humans[30,33-35].

In our model, pigs exhibited clinical deterioration due to pulmonary and systemic emboli, resulting in hypoxia, hypotension, and myocardial infarction. These findings align with existing literature, supporting close monitoring during orthopaedic surgery, particularly surgery involving long bones[2,4,36]. Our findings indicate that combining perioperative ECG with postoperative measurement of troponin-I levels may provide warning of systemic bone marrow embolization. If a patient undergoing orthopaedic surgery develops hypoxia, hypotension, or ECG changes indicative of acute ischemia, bone marrow embolization should be suspected.

Brain infarction resulting from bone marrow emboli was detected in 11 of the 12 pigs that underwent intramedullary nailing but could not be correlated with neurological symptoms as those were masked by anesthesia. The extent of organ damage likely depended on the amount of emboli passing through the pulmonary vasculature, reaching vital organs.

Perioperative TEE detected emboli on the right side of the heart but not the left, contrary to postmortem findings of systemic emboli. TEE detects right-sided emboli during orthopaedic surgery with high sensitivity[23,25,26,37,38] and such findings may predict clinical deterioration[23,24].

Regardless of whether systemic embolic passage through the lungs occurs via arteriovenous shunts or through capillaries, TEE should detect emboli in the pulmonary vein or aorta. However, we were unable to visually detect aortic emboli, even in pigs with significant emboli in the RVOT, suggesting that most emboli were trapped in pulmonary vasculature.

Although not visible on TEE during the experiments, we found emboli in both heart and brain tissue during postmortem examinations. This suggests that emboli can move systemically without intracardiac shunts, as has been also suggested by other studies[39-41]. The failure to detect the systemic embolization using TEE indicates that TEE may not be the optimal modality for this purpose.

High-intensity transient signals shown by perioperative TEE have limitations with regard to distinguishing embolus types. Such signals may represent blood clots, air bubbles, bone marrow emboli, or a combination. However, in our study, bone marrow emboli seemed to have some distinguishing visual characteristics. They were observed before fluid boluses and had a different distribution pattern compared with that of blood clots and air bubbles, as has been described by others[33,42]. Transcranial Doppler ultrasound with frequency modulation may have more promise for detecting systemic perioperative bone marrow emboli in the heart, aorta, or neck vessels[43-45].

The risk of severe multiorgan failure in patients with fat and bone marrow emboli is influenced by immunological factors, embolic burden, affected organs, and compensatory capacity. Perioperative warning signs include ST-segment changes

on ECG, hypotension, and neurological changes. Early detection is crucial as supportive treatment may improve outcomes[3,9].

Susceptibility-weighted MRI is advisable for patients exhibiting neurological changes, and transfer to a neurosurgical center is warranted if increased intracranial pressure is suspected. Early diagnosis may improve survival through organ support[3,9] and, if indicated, neurosurgical decompression[46]. These measures may have contributed to the reduced mortality found in recent compared with older studies[47].

There is no effective pharmacological treatment for fat embolism syndrome following systemic bone marrow embolization, but early fracture fixation combined with embolus-reducing orthopaedic techniques may be preventive[48]. Continuous suction and lavage of the medullary canal can reduce embolic burden[49-51], and measures lowering pressure during reaming may decrease emboli[52].

As observed in our pig model, systemic embolization during femoral nailing is more common than previously thought. The perceived rarity of this condition may be due to insufficient detection methods. Comprehensive clinical studies combining perioperative monitoring, imaging, and neurophysiological testing are needed to improve detection rates and understand implications in patients.

Our study had limitations, including a limited observation time in a small sample. Thus, although systemic emboli were observed in all 12 pigs that underwent intramedullary nailing, the clinical relevance could not be fully elucidated under these constraints. Prolonged observation is necessary to detect complications such as heart failure and cerebral herniation. Also, we conducted extensive histopathological analyses but lacked resources for quantitative analysis correlating embolic number with clinical outcomes.

In conclusion, bilateral femoral intramedullary nailing resulted in clinical lung and systemic emboli, confirmed by biopsies, in all of the animals in our experimental group. TEE detected right-sided but not systemic embolization. Systemic embolization is likely also common in humans. Additional studies are needed to assess strategies for reducing bone marrow emboli and evaluating perioperative and postoperative monitoring and diagnostics. ■

Steinar Kristiansen, MD[1,2]
Anders Hagen Jarmund, MSc[3]
Jonas Hilmo, MD[1,2]
Tom Eirik Mollnes, MD, PhD[4,5]
Martin Leth-Olsen, MD[3,6]
Siri Ann Nyrnes, MD, PhD[3,6]
Bent Aksel Nilsen, RN[1,7]
Renathe Henriksen Grønli, MSc[4]
Bjørn Ove Faldaas, MSc[3,7]
Benjamin Storm, MD, PhD[1,2,7]
Arild Espenes, DVM, PhD[8]
Erik Waage Nielsen, MD, PhD[1,2,7]

[1]Department of Surgery, Nordland Hospital, Bodø, Norway

[2]Institute of Clinical Medicine, University of Tromsø, Tromsø, Norway

[3]Department of Circulation and Medical Imaging (ISB), Faculty of Medicine and Health Sciences, Norwegian University of Science and Technology, Trondheim, Norway

[4]Research Laboratory, Nordland Hospital, Bodø, Norway

[5]Department of Immunology, Oslo University Hospital, University of Oslo, Norway

[6]Children's Clinic, St. Olavs Hospital, Trondheim University Hospital, Trondheim, Norway

[7]Faculty of Nursing and Health Sciences, Nord University, Bodø, Norway

[8]Department of Basic Sciences and Aquatic Medicine, Norwegian School of Veterinary Science, Oslo, Norway

Email for corresponding author: steinarkristiansen@gmail.com

References

1 Weinhouse GL, Parsons PFG. Fat embolism syndrome. 2023. Accessed 2023 Dec 19. https://www.uptodate.com/contents/fat-embolism-syndrome#H8.

2. Huffman JS, Humston C, Tobias J. Fat Embolism Syndrome Revisited: A Case Report and Review of Literature, With New Recommendations for the Anesthetized Patient. AANA J. 2020 Jun;88(3):222-8.

3. Newbigin K, Souza CA, Torres C, Marchiori E, Gupta A, Inacio J, Armstrong M, Peña E. Fat embolism syndrome: State-of-the-art review focused on pulmonary imaging findings. Respir Med. 2016 Apr;113:93-100.

4. Luff D, Hewson DW. Fat embolism syndrome. BJA Educ. 2021 Sep;21(9):322-8.

5. Gavrankapetanović I, Papović A, Jamakosmanović M, Baždar E, Tafro L. Fat Embolism in Orthopedic Surgery. IntechOpen; 2017.

6. Shaikh N. Emergency management of fat embolism syndrome. J Emerg Trauma Shock. 2009 Jan;2(1):29-33.

7. Stump B, Weinhouse G. Fat Embolism Syndrome: Fact or Myth? Curr Trauma Rep. 2016;2(2):66-72.

8. Tsai SHL, Chen CH, Tischler EH, Kurian SJ, Lin TY, Su CY, Osgood GM, Mehmood A, Fu TS. Fat Embolism Syndrome and in-Hospital Mortality Rates According to Patient Age: A Large Nationwide Retrospective Study. Clin Epidemiol. 2022 Aug 19;14:985-96.

9. Kuo KH, Pan YJ, Lai YJ, Cheung WK, Chang FC, Jarosz J. Dynamic MR imaging patterns of cerebral fat embolism: a systematic review with illustrative cases. AJNR Am J Neuroradiol. 2014 Jun;35(6):1052-7.

10 Kristiansen S, Madsen MR, Steen R, Nielsen EW. A young trauma patient with five fractures and multi-organ failure. 2018. Accessed 2023 Dec 19. https://tidsskriftet.no/en/2018/05/noe-laere-av/young-trauma-patient-five-fractures-and-multi-organ-failure.

11. Kellogg RG, Fontes RBV, Lopes DK. Massive cerebral involvement in fat embolism syndrome and intracranial pressure management. J Neurosurg. 2013 Nov;119(5):1263-70.

12. Kawati R, Larsson A. Brain death due to fat embolism - could moderate hypercapnia and prone position be blamed for the tonsillar herniation? Ups J Med Sci. 2013 Nov;118(4):276-8.

13. Berlot G, Bussani R, Shafiei V, Zarrillo N. Fulminant Cerebral Fat Embolism: Case Description and Review of the Literature. Case Rep Crit Care. 2018 Jul 11; 2018:7813175.

14. Wang W, Chen W, Zhang Y, Su Y, Wang Y. Post-traumatic cerebral fat embolism syndrome with a favourable outcome: a case report. BMC Neurol. 2021;21(1):82.

15. Srikanth K, Sundararajan S, Rajasekaran S. Late recovery in cerebral fat embolism. Indian J Orthop. 2014 Jan;48(1):100-3.

16. Oyedeji O, Anusim N, Alkhoujah M, Dabak V, Otrock ZK. Complete Neurologic Recovery of Cerebral Fat Embolism Syndrome in Sickle Cell Disease. Cureus. 2022 Sep 13;14(9):e29111.

17. Kwiatt ME, Seamon MJ. Fat embolism syndrome. Int J Crit Illn Inj Sci. 2013 Jan; 3(1):64-8.

18. Burns JD, Noujaim D, Scott BJ. Susceptibility-Weighted Imaging Diagnosis of Cerebral Fat Embolism. Neurohospitalist. 2017 Jul;7(3):147.

19. Sethi D, Kajal S, Saxena A. Neuroimaging findings in a case of cerebral fat embolism syndrome with delayed recovery. Indian J Crit Care Med. 2015 Nov; 19(11):674-7.

20. Uransilp N, Muengtaweepongsa S, Chanalithichai N, Tammachote N. Fat Embolism Syndrome: A Case Report and Review Literature. Case Rep Med. 2018; 2018:1479850.

21. Wang Y, Si Z, Han J, Cao S. Imaging findings of cerebral fat embolism syndrome: a case report. J Int Med Res. 2020 Sep;48(9):300060520950559.

22. Qi M, Zhou H, Yi Q, Wang M, Tang Y. Pulmonary CT imaging findings in fat embolism syndrome: case series and literature review [Northfield Il]. Clin Med (Lond). 2023 Jan;23(1):88-93.

23. Koessler MJ, Fabiani R, Hamer H, Pitto RP. The clinical relevance of embolic events detected by transesophageal echocardiography during cemented total hip arthroplasty: a randomized clinical trial. Anesth Analg. 2001 Jan;92(1):49-55.

24. Lu K, Xu M, Li W, Wang K, Wang D. A study on dynamic monitoring, components, and risk factors of embolism during total knee arthroplasty. Medicine (Baltimore). 2017 Dec;96(51):e9303.

25. Bisignani G, Bisignani M, Pasquale GS, Greco F. Intraoperative embolism and hip arthroplasty: intraoperative transesophageal echocardiographic study. J Cardiovasc Med (Hagerstown). 2008 Mar;9(3):277-81.

26. Pitto RP, Blunk J, Kössler M. Transesophageal echocardiography and clinical features of fat embolism during cemented total hip arthroplasty. A randomized study in patients with a femoral neck fracture. Arch Orthop Trauma Surg. 2000;120(1-2):53-8.

27. Milroy CM, Parai JL. Fat Embolism, Fat Embolism Syndrome and the Autopsy. Acad Forensic Pathol. 2019 Sep;9(3-4):136-54.

28. Vetrugno L, Bignami E, Deana C, Bassi F, Vargas M, Orsaria M, Bagatto D, Intermite C, Meroi F, Saglietti F, Sartori M, Orso D, Robiony M, Bove T. Cerebral fat embolism after traumatic bone fractures: a structured literature review and analysis of published case reports. Scand J Trauma Resusc Emerg Med. 2021 Mar 12;29(1):47.

29. Eriksson EA, Schultz SE, Cohle SD, Post KW. Cerebral fat embolism without intracardiac shunt: A novel presentation. J Emerg Trauma Shock. 2011 Apr;4(2):309-12.

30. Lovering AT, Elliott JE, Beasley KM, Laurie SS. Pulmonary pathways and mechanisms regulating transpulmonary shunting into the general circulation: an update. Injury. 2010 Nov;41(2):S16-23.

31. Vik SD, Torp H, Follestad T, Støen R, Nyrnes SA. NeoDoppler: New ultrasound technology for continous cerebral circulation monitoring in neonates. Pediatr Res. 2020 Jan;87(1):95-103.

32. Vik A, Jenssen BM, Brubakk AO. Comparison of haemodynamic effects during venous air infusion and after decompression in pigs. Eur J Appl Physiol Occup Physiol. 1994;68(2):127-33.

33. Storm BS, Halvorsen PS, Skulstad H, Dybwik K, Schjalm C, Christiansen D, Wisløff-Aase K, Fosse E, Braaten T, Nielsen EW, Mollnes TE. Open chest and pericardium facilitate transpulmonary passage of venous air emboli. Acta Anaesthesiol Scand. 2021 May;65(5):648-55.

34. Eldridge MW, Dempsey JA, Haverkamp HC, Lovering AT, Hokanson JS. Exercise-induced intrapulmonary arteriovenous shunting in healthy humans. J Appl Physiol (1985). 2004 Sep;97(3):797-805.

35. Boissier F, Razazi K, Thille AW, Roche-Campo F, Leon R, Vivier E, Brochard L, Brun-Buisson C, Mekontso Dessap A. Echocardiographic detection of transpulmonary bubble transit during acute respiratory distress syndrome. Ann Intensive Care. 2015 Mar 24;5(1):5.

36. Sablone S, Cazzato G, Spagnolo L, Berterame C, Mele F, Introna F, Di Fazio A. Post-Trauma Combined Pulmonary Fat and Bone Embolism: Literature Review with Case Presentation. Forensic Sci. 2022;2(2):371-8.

37. Maghrebi S, Cheikhrouhou H, Triki Z, Karoui A. Transthoracic Echocardiography in Fat Embolism: A Real-Time Diagnostic Tool. J Cardiothorac Vasc Anesth. 2017 Jun;31(3):e47-8.

38. Lafont ND, Kalonji MK, Barre J, Guillaume C, Boogaerts JG. Clinical features and echocardiography of embolism during cemented hip arthroplasty. Can J Anaesth. 1997 Feb;44(2):112-7.

39. Byrick RJ, Mullen JB, Mazer CD, Guest CB. Transpulmonary systemic fat embolism. Studies in mongrel dogs after cemented arthroplasty. Am J Respir Crit Care Med. 1994 Nov;150(5 Pt 1):1416-22.

40. Kristiansen S, Storm B, Dahle D, Domaas Josefsen T, Dybwik K, Nilsen BA, Waage-Nielsen E. Intraosseous fluid resuscitation causes systemic fat emboli in a porcine hemorrhagic shock model. Scand J Trauma Resusc Emerg Med. 2021 Dec 20;29(1):172.

41. Nikolić S, Zivković V, Babić D, Djonić D, Djurić M. Systemic fat embolism and the patent foramen ovale—a prospective autopsy study. Injury. 2012 May;43(5):608-12.

42. Wang AZ, Zhou M, Jiang W, Zhang WX. The differences between venous air embolism and fat embolism in routine intraoperative monitoring methods, transesophageal echocardiography, and fatal volume in pigs. J Trauma. 2008 Aug;65(2): 416-23.

43. Silbert BS, Evered LA, Scott DA, Rahardja S, Gerraty RP, Choong PF. Review of transcranial Doppler ultrasound to detect microemboli during orthopedic surgery. AJNR Am J Neuroradiol. 2014 Oct;35(10):1858-63.

44. Kussman BD, Imaduddin SM, Gharedaghi MH, Heldt T, LaRovere K. Cerebral Emboli Monitoring Using Transcranial Doppler Ultrasonography in Adults and Children: A Review of the Current Technology and Clinical Applications in the Perioperative and Intensive Care Setting. Anesth Analg. 2021 Aug 1;133(2):379-92.

45. Banahan C, Rogerson Z, Rousseau C, Ramnarine KV, Evans DH, Chung EML. An in vitro comparison of embolus differentiation techniques for clinically significant macroemboli: dual-frequency technique versus frequency modulation method. Ultrasound Med Biol. 2014 Nov;40(11):2642-54.

46. Couturier C, Dupont G, Vassal F, Boutet C, Morel J. Effectiveness of Decompressive Hemicraniectomy to Treat a Life-Threatening Cerebral Fat Embolism. Case Rep Crit Care. 2019 Feb 28;2019:2708734.

47. He Z, Shi Z, Li C, Ni L, Sun Y, Arioli F, Wang Y, Ammirati E, Wang DW. Single-case metanalysis of fat embolism syndrome. Int J Cardiol. 2021 Dec 15;345:111-7.

48. Adeyinka A, Pierre L. Fat Embolism. StatPearls. StatPearls Publishing; 2023 Jan.

49. Hall JA, McKee MD, Vicente MR, Morison ZA, Dehghan N, Schemitsch CE, Kreder HJ, Petrisor B, Schemitsch EH. Prospective Randomized Clinical Trial Investigating the Effect of the Reamer-Irrigator-Aspirator on the Volume of Embolic Load and Respiratory Function During Intramedullary Nailing of Femoral Shaft Fractures. J Orthop Trauma. 2017 Apr;31(4):200-4.

50. Cox G, Jones E, McGonagle D, Giannoudis PV. Reamer-irrigator-aspirator indications and clinical results: a systematic review. Int Orthop. 2011 Jul;35(7):951-6.

51. Miller AN, Deal D, Green J, Houle T, Brown W, Thore C, Stump D, Webb LX. Use of the Reamer/Irrigator/Aspirator Decreases Carotid and Cranial Embolic Events in a Canine Model. J Bone Joint Surg Am. 2016 Apr 20;98(8):658-64.

52. Timon C, Keady C, Murphy CG. Fat Embolism Syndrome - A Qualitative Review of its Incidence, Presentation, Pathogenesis and Management. Malays Orthop J. 2021 Mar;15(1):1-11.